

that *all* mesons are reabsorbed. A direct measurement of the ratio of photostars (3 prongs) to free mesons produced in emulsion by 315-Mev bremsstrahlung was made by George¹⁰ who found 7.6 when single-meson tracks as well as mesons with associated prongs were included. When photostars of all prongs and neutral mesons are included, the total meson yield is 12% of the total photostar yield. Calculations from Butler's model by George¹⁰ give 8–13%, whereas the optical model gives a much higher (50–60%) meson yield. Reduction of the solid curve by this amount would improve agreement with the lower energy photostar yields, but would account for only approximately half of the 400–500 Mev photostars. Experiments at higher

bremsstrahlung energies would help decide whether the photostar cross section continues to remain high.

ACKNOWLEDGMENTS

We wish to thank Dr. Alvin V. Tollestrup and Mr. William S. MacDonald for assistance in operation of the synchrotron and in making the exposures. The scanning of the plates was materially aided by the careful work of Mrs. Elaine Motta and Miss Kit Wong.

We also wish to thank Professor R. F. Christy for helpful discussions, and Professor R. F. Bacher for his support and encouragement. One of us (C.E.R.) wishes to express his appreciation of the hospitality of the California Institute for extending to him the use of its facilities.

Cosmic-Ray Bursts under Lead at Sea Level*

HUGH CARMICHAEL AND JOHN F. STELJES

Chalk River Laboratories, Atomic Energy of Canada, Limited, Chalk River, Ontario, Canada

(Received July 27, 1956)

The integral size-frequency distributions of ionization bursts near sea level were measured in a thin-walled ($\frac{1}{8}$ inch steel), 8-inch diameter, spherical ion-chamber filled with argon at 50 atmos pressure, under 14 different thicknesses of lead ranging from 0.11 cm to 22 cm. The measurements, along with those already published for the ion chamber with no shield and with a 27-cm lead shield, represent some 15 000 hours of recording. The range of size covered extends from about 3×10^4 to 10^8 ion pairs. In a subsidiary experiment the size-frequency distributions of bursts directly associated with extensive air showers were measured and to these were added, at each thickness of the shield, the bursts due to single μ mesons, protons, and stars derived from the analysis already published. These totals were then subtracted

from the gross size-frequency distributions. The bursts remaining are almost wholly due to the electrons and photons of the soft component and to the radiative and knock-on processes of μ mesons. Transition curves of these bursts (Rossi curves) are given for selected sizes, corresponding (on the average) to showers of 1, 2, 4, 8, \dots , 512 electrons crossing the ion chamber. There is no sign of a second maximum in these transition curves. There is strong evidence that the cascades which give rise to the "first" maximum originate from *single* electrons or photons incident on the lead shield and hence these experimental results are suitable for a straightforward comparison with cascade theory in an energy range extending to some 50 Bev. Indications of a transition effect of the bursts attributed to stars are noted.

1. GENERAL

WE reported in I¹ the cosmic-ray ionization pulses or bursts observed in an unshielded, thin-walled, 8-inch diameter, spherical ion-chamber (volume 4.4 liters, with 50 atmospheres argon at 0°C) at 400 feet above sea level at Deep River, Ontario (lat 46° 06' N, long 70° 30' W). The wall of the ion-chamber was steel, $\frac{1}{8}$ -inch thick. The pulse-recording equipment was capable of dealing, in the same experimental run, with bursts of a range of size of nearly four decades and the bursts due to single cosmic-ray mesons and electrons were measurable. The bursts observed in the ion chamber under a 27-cm-thick shield of lead were also reported in I and a comparison of the two size-frequency distribution curves, unshielded and shielded, permitted

analysis of both curves into separate components representing the size-frequency distributions of the bursts due to single μ mesons, electrons, single protons, stars, extensive showers, and cascades originating in the lead.

In continuation of this work, bursts have been measured with 14 other thicknesses of the lead shield, ranging from 0.11 cm to 22.0 cm, and it is the purpose of this paper to present these observations. It should be noted that the measurements are basic in the sense that there was no preselection of the events by counter telescope or other means, so that the results comprise *all* the ionization bursts that arise, in a spherical vessel, from the omnidirectional flux of the cosmic radiation at the site of the experiment. In a subsidiary experiment the bursts that occurred in coincidence with extensive air showers were directly measured for several thicknesses of the lead shield.

An analysis of the results is given which yields as its principal result a family of transition curves showing

* A preliminary report of some of these measurements was given at the Chicago Meeting of the American Physical Society, November, 1953 [H. Carmichael and J. F. Steljes, Phys. Rev. **93**, 913(A) (1954)].

¹ H. Carmichael and J. F. Steljes, Phys. Rev. **99**, 1542 (1955).

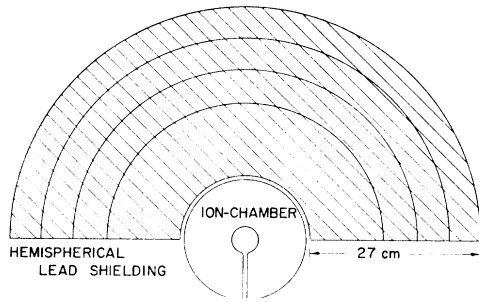


FIG. 1. The 8-inch diameter ion chamber with the 27-cm thick hemispherical lead shield.

the rates of occurrence of electromagnetic cascade bursts (excluding those associated with extensive showers) of any given size (ranging to cascades of 500 electrons) as a function of thickness of the lead shield. These curves are closely analogous to the well-known Rossi² curve originally measured with counters. Another result of the analysis indicates a transition effect under lead associated with the bursts arising from stars.

2. APPARATUS

The ion chamber, recording methods, and calibration have already been described in I.

The lead shielding was hemispherical and is indicated in Fig. 1. Thicknesses 0.110, 0.262, 0.370, 0.67, 1.35, 2.02, 2.70, 3.36, 4.04, 5.39, and 6.73 cm (these are not shown in Fig. 1) were formed by successively adding closely fitting hemispheres, the weight resting on the ion chamber. The 12-cm shield was a single hemisphere which replaced the thinner ones and had a 1/4-inch gap between it and the ion chamber. The 17-, 22-, and 27-cm thicknesses were formed by adding in succession single hemispheres, the outer one weighing more than 1000 lb.

The choice of hemispherical rather than spherical shielding was given careful consideration before the experiment was started. It was hoped, because of the greater convenience, that a valid experiment could be performed with hemispherical shielding. Therefore, some 2000 hours were devoted to making two test runs, one with a lead hemisphere of moderate thickness (4.04 cm) surrounding the lower half of the ion chamber, and one with the ion chamber resting in contact with a horizontal lead plate, one meter square and 5 cm thick. The results are plotted in Fig. 2 (curves (c) and (b), respectively) in comparison with the integral size-frequency distribution of bursts in the unshielded ion chamber [curve (a)] already reported in I. Also shown in Fig. 2 is the result obtained (see below) with the 4.04-cm lead hemisphere above the ion chamber [curve (d)].

² B. Rossi, Z. Physik. 82, 151 (1933); Rend. reale accad. naz. Lincei. 17, 1073 (1933).

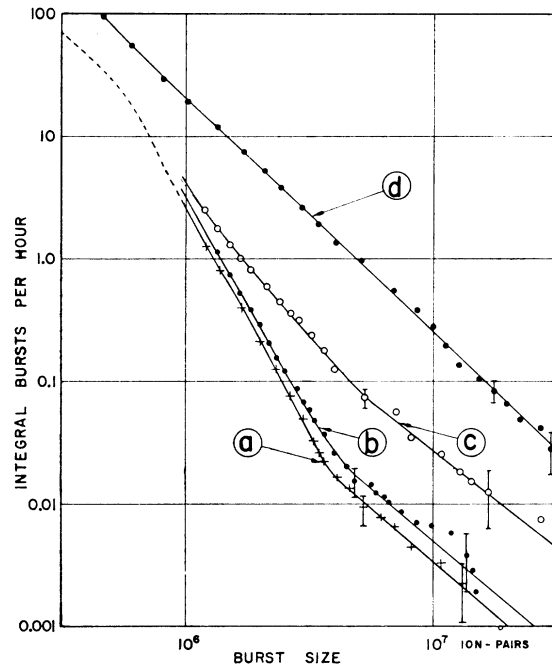


FIG. 2. The size-frequency distributions of the larger bursts: (a) unshielded ion chamber; (b) with a horizontal plate of lead 5-cm thick and 1-meter square below and in contact with the ion chamber; (c) with the lower half of the ion chamber in a closely fitting lead hemisphere 4.04 cm thick; (d) with the same lead hemisphere covering the upper half of the ion chamber.

In Fig. 2, at burst size 10⁷ ion pairs the integral rates per 1000 hours are

- (a) ion chamber unshielded, 3 ± 2;
- (b) with lead plate below, 5 ± 2;
- (c) with 4.04 cm lead hemisphere below, 26 ± 10;
- (d) with 4.04 cm lead hemisphere above, 250 ± 100.

The increase produced by the hemisphere surrounding the lower half of the ion chamber is significant but the increase seen with the flat plate below is small and within the experimental error of the observations. It was concluded that the increased rate observed with a lead hemisphere surrounding the lower half of the ion chamber must be attributed to cascades generated in a forward and downward direction by particles intersecting the rim of the hemisphere. Therefore, especially to be avoided was an experiment in which the lower half of the ion chamber was permanently surrounded by a thick lead hemisphere. Further, the result with the flat lead plate showed that true backscattering effects were not large. So it was decided that the measurements would be made with the lower half of the ion chamber completely unshielded. At this time the apparatus was not capable of measuring with good accuracy bursts smaller than those plotted in Fig. 2, but certainly no large backscattering effects in the region of smaller bursts were indicated.

TABLE I. Integral size-frequency distributions of bursts under lead. The figures are the logarithms to base ten of computed rates per hour (see text). Where the computed figures differ by more than $\pm 5\%$, or by more than the statistical error, from the readings taken off the measured curves, corrections are given.

log ₁₀ (size in ion pairs)	Duration of run (hours)															
	4483	...	960	...	381	269	360	201	398	289	...	1453	559	667	561	1852
	0	0.110	0.262	0.360	0.67	1.35	2.02	2.70	3.36	4.04	5.39	6.73	12.0	17.0	22.0	27.0
4.3	4.52	4.35	4.31
4.4	4.46	4.32	4.28
4.5	4.41	4.27	4.23
4.6	4.35	4.21	4.17
4.7	4.28	4.31	4.31	4.31	4.30	4.27	4.23	4.21	4.19	4.18	4.16	4.15	4.14	4.12	4.11	4.10
4.8	4.02	4.09	4.09	4.09	4.09	4.04	4.01	3.97	3.96	3.94	3.92	3.91	3.88	3.87	3.86	3.85
4.9	3.66	3.77	3.80	3.81	3.82	3.75	3.70	3.66	3.62	3.59	3.56	3.54	3.51	3.49	3.48	3.47
5.0	3.32	3.50	3.53	3.56	3.59	3.52	3.46	3.41	3.36	3.32	3.27	3.24	3.19	3.17	3.15	3.14
5.1	2.98	3.20	3.27	3.32	3.37	3.31	3.23	3.17	3.11	3.06	3.00	2.96	3.89	2.86	2.84	2.83
5.2	2.62	2.90	2.99	3.05	3.14	3.11	3.02	2.96	2.90	2.83	2.75	2.68	2.60	2.56	2.53	2.51
5.3	2.27	2.60	2.70	2.79	2.91	2.92	2.84	2.77	2.69	2.61	2.52-0.04	2.44	2.33	2.28	2.25	2.23
5.4	2.04	2.31	2.44-0.04	2.52-0.03	2.69	2.74	2.66	2.60	2.52-0.03	2.43-0.03	2.32-0.04	2.24-0.03	2.11	2.06	2.01	1.99
5.5	1.85	2.05	2.17-0.03	2.26-0.03	2.47	2.56	2.50	2.44	2.35-0.03	2.26-0.03	2.14-0.04	2.05	1.92	1.86	1.81	1.77
5.6	1.67	1.79	1.91	1.99	2.23	2.39	2.35	2.28	2.18	2.09	1.96-0.03	1.87	1.73	1.67	1.62	1.58
5.7	1.47	1.55	1.65	1.73+0.03	1.99+0.03	2.20	2.17	2.11	2.01	1.92	1.78-0.03	1.67	1.54	1.48	1.42	1.38
5.8	1.21	1.26	1.35+0.03	1.43+0.05	1.73+0.02	1.98	1.98	1.92	1.83	1.73	1.57	1.47	1.33	1.27	1.22	1.18
5.9	0.80	0.85+0.07	0.95+0.09	1.04+0.10	1.42+0.03	1.75	1.77	1.72	1.62	1.51	1.33	1.22	1.08	1.02-0.03	0.99	0.96
6.0	0.43	0.47+0.09	0.57+0.13	0.67+0.14	1.11+0.04	1.53	1.56	1.51	1.43	1.32	1.12	0.99	0.85	0.81-0.04	0.78-0.03	0.76
6.1	0.08	0.12+0.07	0.19+0.18	0.33+0.13	0.78+0.06	1.28	1.34	1.30	1.23	1.13	0.91	0.79	0.64	0.61-0.03	0.59	0.57
6.2	1.74	...	1.87+0.17	...	0.49+0.04	1.04	1.12	1.09	1.03	0.93	...	0.59	0.45	0.41-0.02	0.40	0.39
6.3	1.39	...	1.52+0.19	...	0.14+0.10	0.77	0.89	0.87	0.83	0.74	...	0.38	0.26	0.23	0.22	0.22
6.4	2.94	...	1.15+0.20	...	1.80+0.14	0.49	0.66	0.66	0.62	0.55	...	0.21	0.07	0.05	0.04	0.04
6.5	2.47	...	2.83+0.19	...	1.48+0.16	0.20	0.43	0.46	0.41	0.35	...	0.02	1.88	1.87	1.86	1.85
6.6	2.11	...	2.63	...	1.19+0.16	1.92	0.20	0.25	0.21	0.16	...	1.84	1.71	1.69	1.68	1.68
6.7	3.88	...	2.47	...	2.93+0.15	1.65+0.05	1.96	0.04	0.00	1.97	...	1.65	1.53	1.52	1.51	1.50
6.8	3.69	...	2.32	...	2.71+0.13	1.38+0.08	1.73	1.83	1.79	1.77	...	1.47	1.36	1.35	1.34	1.33
6.9	3.52	...	2.16	...	2.52+0.08	1.11+0.12	1.50	1.62	1.59	1.58	...	1.29	1.19	1.17	1.16	1.16
7.0	3.34	...	2.12	...	2.35+0.04	2.86+0.14	1.26	1.41	1.40	1.39	...	1.11	1.01	1.00	2.99	2.98
7.5	4.47	...	3.32	...	3.65	3.94	2.20	2.37	2.30	2.38	...	2.19	2.14	2.13	2.12	2.12

3. RESULTS

(a) All Bursts

The long runs (varying from 200 to nearly 2000 hours each, depending upon the thickness of lead) necessary to establish the rates of occurrence of the larger bursts

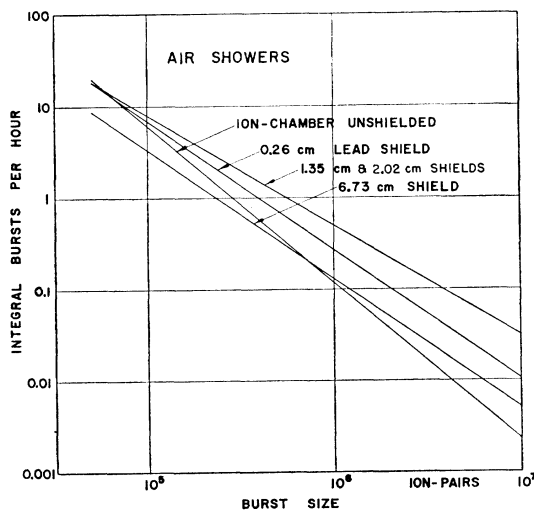


FIG. 3. The size-frequency distributions of the bursts that occur in coincidence with extensive air showers, for the ion chamber unshielded and with 4 representative thicknesses of the hemispherical lead shield.

(the sizes from 10^6 to 10^8 ion pairs) were made with the vibrating reed equipment (see I), and the smaller bursts were measured in shorter runs using the electrometer tube equipment with frequent recycling of shield thicknesses. The measured rates were corrected for barometer effect to a pressure of 997 mb by using coefficients of -3% per cm Hg for bursts of less than 10^6 ion pairs and -10% per cm Hg for all larger bursts. A small discontinuity at size 10^5 ion pairs occasionally introduced by this treatment of the data disappeared in the graphical smoothing process described in the next paragraph (also the shorter runs for measuring the smaller bursts were always made at times when the barometric pressure was near its mean value).

The corrected observations, including those with no lead above the ion chamber, were plotted in the form of integral size-frequency distributions on a very large sheet of graph paper. Smooth curves, removing only minor irregularities, were drawn through the experimental points. In regions where the curves for successive thicknesses of the shield were closely spaced, the delineation of each individual curve was to some extent assisted by the shape of its nearest neighbors.

This graph is too large and detailed for satisfactory reproduction and the original experimental points are too numerous for economical tabulation but all of the curves may be reproduced to within $\pm 5\%$ or to within the limits of the statistical error, whichever is the

greater, by means of Table I. The figures in Table I are the sums of the smoothed components used in the analysis described in Sec. 4. In several places, where these sums differed by more than 5% from the original smoothed curves, the corrections required to obtain these latter curves are given. The agreement of five of the curves represented in Table I with the original experimental points may be inspected in Figs. 3 and 5 of I and in Figs. 4, 7, and 8 in this paper.

(b) Bursts Associated with Extensive Showers

The ion chamber was gated by a 30-inch-diameter ion chamber placed at the same level about 3 meters away as already described in I. Only those bursts in the 8-inch ion chamber which were associated with bursts in the 30-inch ion chamber of size corresponding to at least 4 extensive shower particles intersecting that ion chamber were recorded. Measurements were made with no shield (see Fig. 4 of I) and with 0.26 (see Fig. 8 of this paper), 0.67, 1.35, 2.02 (see Fig. 4 of this paper), 4.04, and 6.73-cm shields. The durations of these runs (from 50 to 300 hours each) were selected to establish the size-frequency distributions of these bursts with accuracy no more than sufficient for analysis of the main curves. The experimental observations at each thickness of lead were approximated within the experimental errors by straight (power law) lines, five of which are shown in Fig. 3. At and beyond 12 cm of lead these bursts were negligible (less than 1%) in comparison with the gross rates. For the analysis described in the following section, for those thicknesses of the shield where the bursts due to extensive showers were not measured, interpolated curves were drawn.

4. ANALYSIS

(a) Transition Curves of Electromagnetic Cascades in Lead

The component size-frequency distributions of the bursts due to single μ mesons, single protons, and stars were derived in I for the zero and 27-cm shield thicknesses by analysis of the gross distribution curves. In that analysis it was taken that the rates of these bursts decreased exponentially with increasing thickness of lead and the absorption coefficient, $4.7 \times 10^{-3} \text{ g}^{-1} \text{ cm}^2$, was found for the protons and assumed for the stars. For mesons the value $0.38 \times 10^{-3} \text{ g}^{-1} \text{ cm}^2$ was assumed. It follows that the proton, star, and μ -meson bursts can be computed for each of the other thicknesses of the lead shield. Hence, for each thickness of the lead shield the sum of the measured (or interpolated) bursts due to extensive showers and the computed bursts due to protons, stars, and μ mesons was found and subtracted from the gross measured size-frequency distribution. The resulting integral distributions, attributed to bursts caused by electron-photon cascades, were plotted and

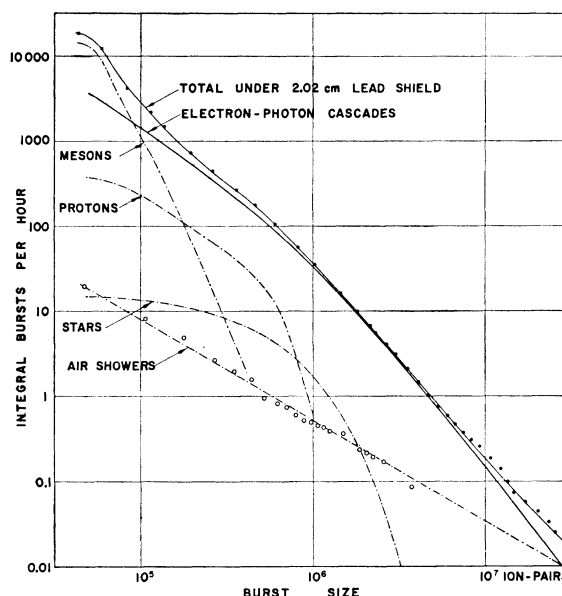


FIG. 4. The smoothed size-frequency distribution of bursts caused by electromagnetic cascades under a 2.02-cm lead shield, obtained by subtracting the four component distributions shown by broken lines from the measured total distribution: the full line through the experimental points is the sum of all five components.

curves drawn smoothing only the minor irregularities of adjacent points. Most of these new curves were quite free from local bulges or discontinuities of slope,

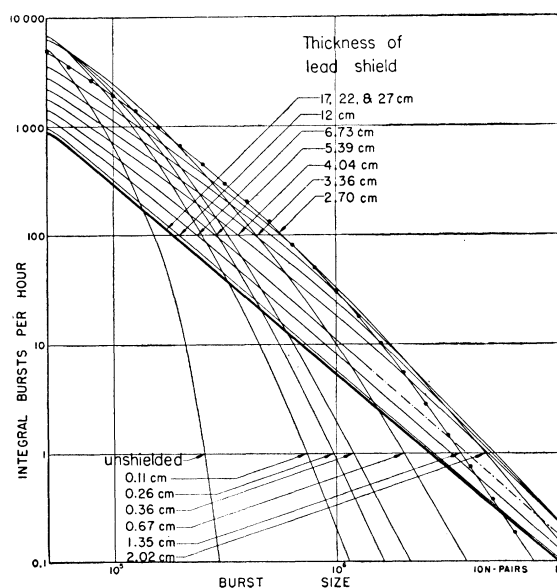


FIG. 5. The smoothed size-frequency distributions of bursts caused by electromagnetic cascades for all the thicknesses of the lead shield. The points shown on the curve for the 1.35-cm-thick shield are not the original experimental readings but derive from the readings taken from the slightly smoothed curve first drawn through the experimental points. These points are given to indicate the amount of additional smoothing introduced in this step of the analysis. Note added in proof.—The 2.70 cm arrow should be lengthened to the next adjacent curve.

³ W. L. Kraushaar, Phys. Rev. 76, 1045 (1949).

TABLE II. Integral size-frequency distributions of bursts attributed to electron-photon cascades. The figures are the logarithms to base ten of the rates per hour.

\log_{10} (size in ion pairs)	Thickness of lead shield (cm)															
	0	0.110	0.262	0.360	0.67	1.35	2.02	2.70	3.36	4.04	5.39	6.73	12.0	17.0	22.0	27.0
4.7	3.72	3.84	3.84	3.84	3.80	3.68	3.56	3.45	3.35	3.26	3.16	3.08	2.99	2.96	2.95	2.94
4.8	3.48	3.68	3.69	3.69	3.69	3.56	3.44	3.33	3.23	3.13	3.03	2.94	2.85	2.82	2.81	2.80
4.9	3.10	3.46	3.50	3.52	3.54	3.42	3.30	3.19	3.09	2.99	2.88	2.78	2.68	2.64	2.63	2.62
5.0	2.72	3.23	3.29	3.34	3.39	3.27	3.16	3.05	2.95	2.85	2.73	2.62	2.50	2.47	2.46	2.45
5.1	2.39	2.96	3.07	3.14	3.21	3.14	3.02	2.91	2.81	2.70	2.58	2.46	2.33	2.30	2.29	2.28
5.2	1.90	2.66	2.81	2.90	3.02	2.98	2.87	2.77	2.66	2.56	2.42	2.29	2.16	2.12	2.11	2.10
5.3	1.21	2.34	2.52	2.63	2.81	2.82	2.72	2.63	2.52	2.41	2.26	2.13	1.99	1.95	1.94	1.93
5.4	0.10	1.99	2.21	2.34	2.58	2.65	2.56	2.48	2.36	2.25	2.09	1.96	1.81	1.77	1.76	1.75
5.5	...	1.62	1.88	2.04	2.34	2.47	2.41	2.32	2.21	2.09	1.92	1.79	1.64	1.60	1.59	1.58
5.6		1.23	1.53	1.72	2.09	2.30	2.25	2.17	2.05	1.93	1.75	1.61	1.46	1.43	1.42	1.41
5.7		0.80	1.17	1.38	1.84	2.11	2.08	2.01	1.89	1.77	1.58	1.44	1.29	1.25	1.24	1.23
5.8		0.34	0.78	1.02	1.57	1.91	1.91	1.84	1.73	1.60	1.40	1.26	1.11	1.08	1.07	1.06
5.9		1.83	0.37	0.65	1.29	1.70	1.72	1.66	1.56	1.43	1.22	1.08	0.94	0.91	0.90	0.89
6.0		1.30	1.94	0.29	0.99	1.48	1.52	1.47	1.39	1.26	1.03	0.90	0.76	0.73	0.72	0.71
6.1		2.76	1.50	1.91	0.67	1.25	1.31	1.27	1.20	1.09	0.85	0.72	0.58	0.56	0.55	0.54
6.2		...	1.06	...	0.35	1.00	1.09	1.06	1.01	0.90	...	0.54	0.40	0.38	0.37	0.36
6.3		...	2.61	...	0.01	0.74	0.86	0.86	0.81	0.72	...	0.36	0.23	0.21	0.20	0.19
6.4		...	2.16	...	1.66	0.46	0.63	0.65	0.60	0.53	...	0.19	0.06	0.04	0.03	0.02
6.5			3.72	...	1.30	0.16	0.40	0.44	0.40	0.34	...	0.01	1.88	1.87	1.86	1.85
6.6			2.94	1.86	0.16	0.23	0.19	0.15	...	1.83	1.71	1.69	1.68	1.67
6.7				...	2.56	1.56	1.92	0.02	1.98	1.95	...	1.65	1.53	1.52	1.51	1.50
6.8				...	2.19	1.26	1.67	1.80	1.77	1.76	...	1.47	1.36	1.35	1.34	1.33
6.9					3.80	2.94	1.42	1.58	1.57	1.56	...	1.29	1.19	1.17	1.16	1.15
7.0					3.40	2.62	1.17	1.36	1.36	1.35	...	1.11	1.01	1.00	2.99	2.98
7.1					...	2.29	2.91	1.14	1.15	1.15	...	2.93	2.84	2.83	2.82	2.81
7.2						3.96	2.65	2.92	2.94	2.95	...	2.75	2.67	2.65	2.64	2.63
7.3						3.62	2.38	2.70	2.73	2.74	...	2.56	2.49	2.48	2.47	2.46
7.4						3.29	2.12	2.48	2.52	2.53	...	2.38	2.32	2.31	2.30	2.29
7.5						...	3.85	2.24	2.30	2.32	...	2.19	2.14	2.13	2.12	2.11

as shown for example in Fig. 4, but the curves for the four thinnest shields each had a bulge in the region of size corresponding to the bursts from stars. This bulge can be seen in Fig. 8 for the 0.26-cm shield.

It was assumed that this bulge found in these curves at small thicknesses of lead was not caused by electron-photon cascade bursts but belonged to a superimposed effect and the curves were redrawn as shown, for example, in Fig. 8 omitting the bulge. The bursts omitted in this way were allocated to the stars as discussed below in 4(b).

All the integral distribution curves found in this way are shown in Fig. 5 and may be replotted from the coordinates given in Table II. On one of the curves of Fig. 5 (for the 1.35-cm shield) the points through which the curve was drawn are also shown. It should be noted here that the accuracy of many of the curves of Fig. 5 over most of their range is comparable with the accuracy of the original gross readings. This may be seen by examination of Fig. 4 where it is evident that the amount subtracted is less than 20% except near the two ends of the curve. Further, even if the corrections to the four thinnest shields for bursts ascribed to stars

had not been made, the aspect of the family of curves in Fig. 5 would have remained essentially the same.

The next step was the conversion of the integral readings of Table II to their exact differential equivalents given in Table III. This was done directly from the integral logarithmic graphs of Fig. 5 by using the relation

$$\log_{10}(dI/dS) = \log_{10} \tan \theta + \log_{10} I - \log_{10} S - 5.0,$$

where dI/dS is the rate per hour of bursts of size S , per 10^5 ion-pair interval, and θ is the angle of slope of the graph at size S ion pairs such that $\log dI/\log dS = \tan \theta$. Transition curves are given by the successive rows of Table III and are plotted in Fig. 6, where each curve shows the absolute rate of occurrence in the ion chamber, of bursts of exactly a certain size, per 10^5 ion-pair interval, as a function of the thickness of the lead shield.

(b) Evidence for a Transition Effect of Bursts Associated with Star Processes

The bursts identified in I as arising from star processes occurring in the unshielded ion chamber were character-

TABLE III. Differential size-frequency distributions of bursts attributed to electron-photon cascades. The figures are the logarithms to base ten of the rates per hour per size interval of 10^6 ion pairs.

\log_{10} (size in ion pairs)	Thickness of lead shield (cm)															
	0	0.110	0.262	0.360	0.67	1.35	2.02	2.70	3.36	4.04	5.39	6.73	12.0	17.0	22.0	27.0
4.7	4.27	4.24	4.22	4.20	4.14	4.02	3.90	3.79	3.69	3.60	3.50	3.42	3.33	3.30	3.29	3.28
4.8	4.14	4.20	4.16	4.11	4.04	3.89	3.77	3.66	3.56	3.48	3.41	3.33	3.29	3.26	3.25	3.24
4.9	3.70	3.92	3.88	3.86	3.82	3.67	3.55	3.42	3.34	3.24	3.16	3.08	3.02	2.98	2.97	2.96
5.0	3.32	3.62	3.62	3.64	3.61	3.42	3.31	3.20	3.10	3.01	2.91	2.83	2.74	2.71	2.70	2.69
5.1	2.97	3.32	3.34	3.38	3.39	3.20	3.08	2.96	2.87	2.78	2.67	2.59	2.47	2.44	2.43	2.42
5.2	2.44	2.96	3.05	3.11	3.14	2.99	2.85	2.73	2.62	2.54	2.43	2.32	2.20	2.16	2.15	2.14
5.3	1.89	2.56	2.71	2.79	2.85	2.74	2.61	2.51	2.39	2.30	2.17	2.05	1.93	1.89	1.88	1.87
5.4	0.96	2.15	2.32	2.42	2.54	2.47	2.35	2.26	2.14	2.05	1.92	1.80	1.65	1.61	1.60	1.59
5.5	...	1.69	1.92	2.05	2.24	2.21	2.10	2.02	1.90	1.80	1.65	1.53	1.38	1.34	1.33	1.32
5.6		1.24	1.49	1.64	1.90	1.97	1.84	1.76	1.66	1.54	1.39	1.25	1.10	1.07	1.06	1.05
5.7		0.75	1.04	1.22	1.57	1.70	1.62	1.53	1.40	1.29	1.12	0.98	0.83	0.79	0.78	0.77
5.8		0.21	0.58	0.78	1.21	1.43	1.38	1.28	1.15	1.03	0.85	0.72	0.55	0.52	0.51	0.50
5.9		$\bar{1}.65$	0.11	0.33	0.87	1.14	1.12	1.03	0.89	0.77	0.57	0.44	0.28	0.25	0.24	0.23
6.0		$\bar{1}.02$	$\bar{1}.59$	$\bar{1}.86$	0.48	0.85	0.84	0.70	0.64	0.50	0.31	0.16	0.00	$\bar{1}.97$	$\bar{1}.96$	$\bar{1}.95$
6.1		...	$\bar{1}.06$	$\bar{1}.38$	0.08	0.55	0.54	0.49	0.39	0.24	0.02	$\bar{1}.88$	$\bar{1}.72$	$\bar{1}.70$	$\bar{1}.69$	$\bar{1}.68$
6.2		$\bar{1}.67$	0.21	0.24	0.18	0.11	$\bar{1}.96$...	$\bar{1}.59$	$\bar{1}.44$	$\bar{1}.42$	$\bar{1}.41$	$\bar{1}.40$
6.3		$\bar{1}.25$	$\bar{1}.88$	$\bar{1}.93$	$\bar{1}.87$	$\bar{1}.81$	$\bar{1}.69$...	$\bar{1}.31$	$\bar{1}.17$	$\bar{1}.15$	$\bar{1}.14$	$\bar{1}.13$
6.4		$\bar{2}.81$	$\bar{1}.51$	$\bar{1}.60$	$\bar{1}.56$	$\bar{1}.51$	$\bar{1}.40$...	$\bar{1}.04$	$\bar{2}.90$	$\bar{2}.88$	$\bar{2}.87$	$\bar{2}.86$
6.5		$\bar{2}.36$	$\bar{1}.14$	$\bar{1}.28$	$\bar{1}.25$	$\bar{1}.22$	$\bar{1}.13$...	$\bar{2}.77$	$\bar{2}.62$	$\bar{2}.61$	$\bar{2}.60$	$\bar{2}.59$
6.6		$\bar{3}.91$	$\bar{2}.74$	$\bar{2}.96$	$\bar{2}.94$	$\bar{2}.91$	$\bar{2}.83$...	$\bar{2}.49$	$\bar{2}.35$	$\bar{2}.33$	$\bar{2}.32$	$\bar{2}.31$
6.7		$\bar{3}.44$	$\bar{2}.35$	$\bar{2}.61$	$\bar{2}.65$	$\bar{2}.60$	$\bar{2}.56$...	$\bar{2}.21$	$\bar{2}.07$	$\bar{2}.06$	$\bar{2}.05$	$\bar{2}.04$
6.8		$\bar{4}.96$	$\bar{3}.94$	$\bar{2}.27$	$\bar{2}.33$	$\bar{2}.91$	$\bar{2}.26$...	$\bar{3}.93$	$\bar{3}.80$	$\bar{3}.79$	$\bar{3}.78$	$\bar{3}.77$
6.9		$\bar{4}.47$	$\bar{3}.54$	$\bar{3}.93$	$\bar{2}.03$	$\bar{3}.98$	$\bar{3}.96$...	$\bar{3}.65$	$\bar{3}.53$	$\bar{3}.51$	$\bar{3}.50$	$\bar{3}.49$
7.0		$\bar{3}.12$	$\bar{3}.58$	$\bar{3}.71$	$\bar{3}.67$	$\bar{3}.65$...	$\bar{3}.37$	$\bar{3}.25$	$\bar{3}.24$	$\bar{3}.23$	$\bar{3}.22$
7.1		$\bar{4}.70$	$\bar{3}.23$	$\bar{3}.39$	$\bar{3}.37$	$\bar{3}.36$...	$\bar{3}.08$	$\bar{4}.98$	$\bar{4}.97$	$\bar{4}.96$	$\bar{4}.95$
7.2		$\bar{4}.29$	$\bar{4}.87$	$\bar{3}.07$	$\bar{3}.06$	$\bar{3}.05$...	$\bar{4}.80$	$\bar{4}.71$	$\bar{4}.69$	$\bar{4}.68$	$\bar{4}.67$
7.3		$\bar{5}.85$	$\bar{4}.51$	$\bar{4}.75$	$\bar{4}.75$	$\bar{4}.77$...	$\bar{4}.52$	$\bar{4}.43$	$\bar{4}.42$	$\bar{4}.41$	$\bar{4}.40$
7.4		$\bar{5}.41$	$\bar{4}.14$	$\bar{4}.44$	$\bar{4}.45$	$\bar{4}.46$...	$\bar{4}.23$	$\bar{4}.16$	$\bar{4}.15$	$\bar{4}.14$	$\bar{4}.13$
7.5		$\bar{5}.77$	$\bar{4}.11$	$\bar{4}.13$	$\bar{4}.15$...	$\bar{5}.96$	$\bar{5}.88$	$\bar{5}.87$	$\bar{5}.86$	$\bar{5}.85$

ized by a frequency of occurrence which was an exponential function of size. Under 27 cm of lead the star bursts were obscured by the more numerous electronic cascade bursts originating in the lead. Under 12 cm of lead, as shown in Fig. 7, the star component is detectable but it amounts, at the most favorable point on the distribution curve, to only $14 \pm 5\%$ of the gross rate. On the basis of this observation it was assumed in I that the star bursts had an absorption mean free path of 215 g cm^{-2} equal to that found for the proton component.

Now, as has just been mentioned above, with the four thinnest lead shields (0.11 to 0.67 cm) in the general region of size of the star bursts there are some bursts, as indicated for example by the shaded areas in Fig. 8, that have not been included with the electronic cascades. These extra bursts appear to have an exponential size-frequency distribution very similar to that of the star component. In fact, if the star component is increased by 50% in Fig. 8, most of the discrepancy disappears. A still better fit may be obtained by adding an exponential with a slightly greater relaxation length to represent the extra bursts. For the

thicknesses of lead in which these extra bursts are visible, their number appears to increase in proportion with thickness so that at 0.67 cm we find an increase approaching 100% . The effect, unfortunately, cannot be followed in these experiments beyond 0.67 cm of lead because of the increasing numbers of bursts due to electronic cascades.

Though surprisingly large and sudden as measured in our experiments, the above effect is probably to be identified with the known⁴ transition effect of star-producing cosmic radiation in lead. We do not know how much of it may be due to the production of additional stars in the gas and how much, if any, is in the form of small showers directly emitted by the lead.

5. DISCUSSION

(a) Average Burst Size Produced by Particles at Minimum Ionization

Since the results of cascade shower theory are given in terms of the numbers of particles in a shower, it is of

⁴ Schopper, Hocker, and Kuhn, Phys. Rev. **82**, 444 (1951), and references therein.

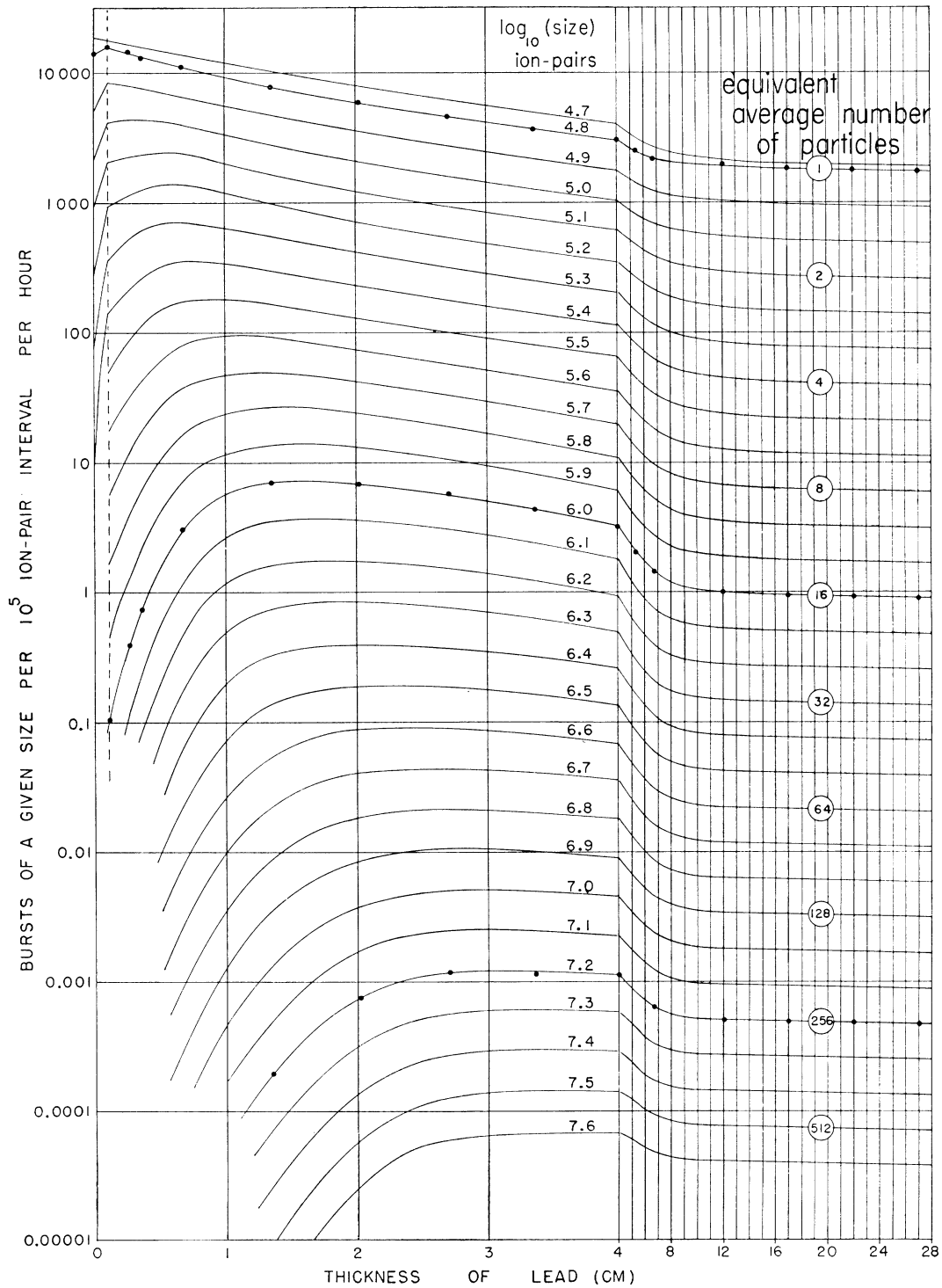


FIG. 6. The rates of occurrence per hour of bursts of different given sizes per 10^5 ion-pair size interval as a function of thickness of the lead shield. The circled number on each third curve indicates the average number of electrons crossing the ion chamber. Note the change of scale on the abscissa at thickness 4 cm of lead. Three typical sets of the points through which these curves were drawn are shown.

interest now to estimate the average number of electron tracks at minimum ionization in the ion chamber corresponding to a cascade burst of given size. The most

probable burst size produced by single relativistic μ mesons intersecting the ion chamber is obtainable from Fig. 9 of I. We shall take this size to be exactly at 4.8

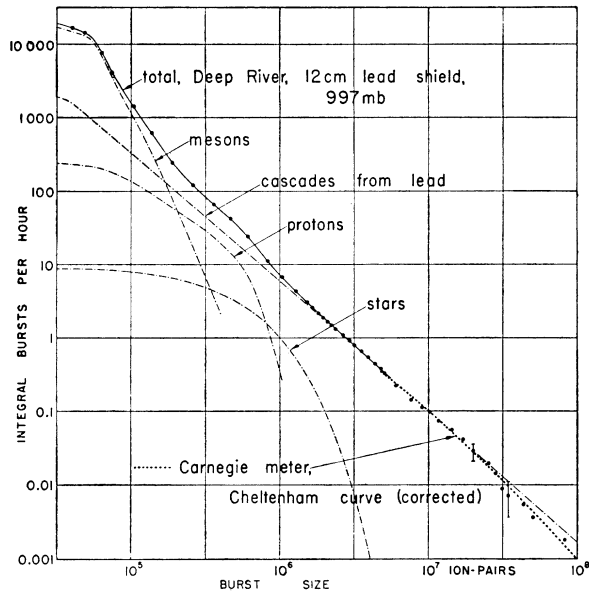


FIG. 7. The size-frequency distribution of bursts under a 12-cm lead shield. The full curve through the experimental points is the sum of the four labelled component distributions indicated by dash dot lines. The dotted line in the region of large bursts is the Cheltenham Carnegie Meter curve, corrected for underestimation of the smaller bursts in their measurements, and compared with our measurements on the basis of the independent calibrations of both ion chambers in terms of the average pulse size of single electrons at minimum ionization intersecting the spherical ion chambers.

on the logarithmic abscissa, corresponding to 6.3×10^4 ion pairs (as already discussed fully in I, these figures are given without correcting for the current carried by the positive ions in the ion chamber which amounts to an additional 11% on the average).

This figure may be checked against the calibration of the Carnegie ion chamber at Cheltenham by comparing the burst rates measured under 12 cm of lead. The comparison is very satisfactory as shown in Fig. 7. The Cheltenham data were represented by a smooth calculated set of points for mesons of spin 0 taken from Table II, page 327 of a paper by Lapp.⁵ Lapp's treatment of the Cheltenham data on pages 324 and 325 was reversed to correspond with our curve by multiplying the rates by 3600 to bring them to bursts per hour and by 324 to correspond with the area of our ion chamber. A calculated size-frequency distribution was used rather than the Cheltenham experimental points because it introduced an appropriate correction of the experimental data for the well-known underestimation of the rates of occurrence of the smaller bursts measured by the Carnegie Meter. The fit of the Cheltenham points with this calculated curve may be seen in Fig. 6 on page 329 of Lapp's paper.

⁵ R. E. Lapp, Phys. Rev. **69**, 321 (1946). For a more recent assessment of this calculation using spin $\frac{1}{2}$, see E. F. Fahy, Phys. Rev. **83**, 413 (1951).

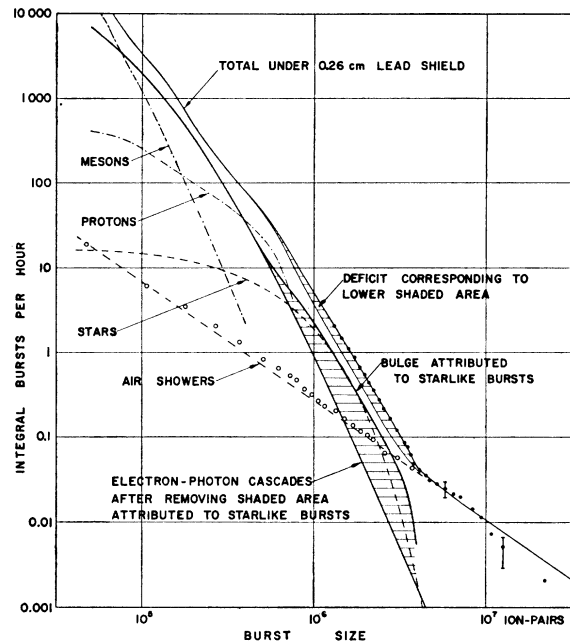


FIG. 8. The size-frequency distribution of bursts under a 0.26-cm lead shield. The open-circle experimental points represent bursts that occur in coincidence with air showers. The routine addition of the meson, proton, star and air-shower components and subtraction from the total, yields an electron-photon cascade component that is not perfectly smooth as indicated by the upper edge of the shaded bulge. When this component curve is smoothed to the lower edge of the shaded area the sum of the five components is less than the measured total by the amount labelled "deficit" on the uppermost curve. This deficit can be removed by alteration of the star distribution as described in the text.

(b) Bursts Associated with Extensive Air Showers

Although the bursts that occur in coincidence with extensive air showers have not been very precisely measured, the general character of their behavior under increasing thicknesses of lead can be seen in Fig. 3. It should be noted that, in the case of the unshielded ion chamber and with shields of thickness less than 2 cm of lead (as may be seen, for example, in Fig. 8), the large burst end of the size-frequency distribution of the air shower bursts is visible in the gross size-frequency distribution curve. The largest bursts that occur seem all to be caused by air showers.

At each thickness of lead the size-frequency distribution of the air shower bursts has been approximated by a power-law curve. The exponent of this power law is 1.73 with the ion-chamber unshielded. It decreases rapidly to about 1.2 for thicknesses 1.35 cm and 2.02 cm of lead, by pivoting about a point at the small size end where the bursts are those produced by single particles intersecting the ion chamber. With thicker lead the slope tends to increase again, and bursts of all sizes become less frequent. The variation of the rate of occurrence of bursts of given size as a function of thickness of shield obtained from Fig. 3 by the same

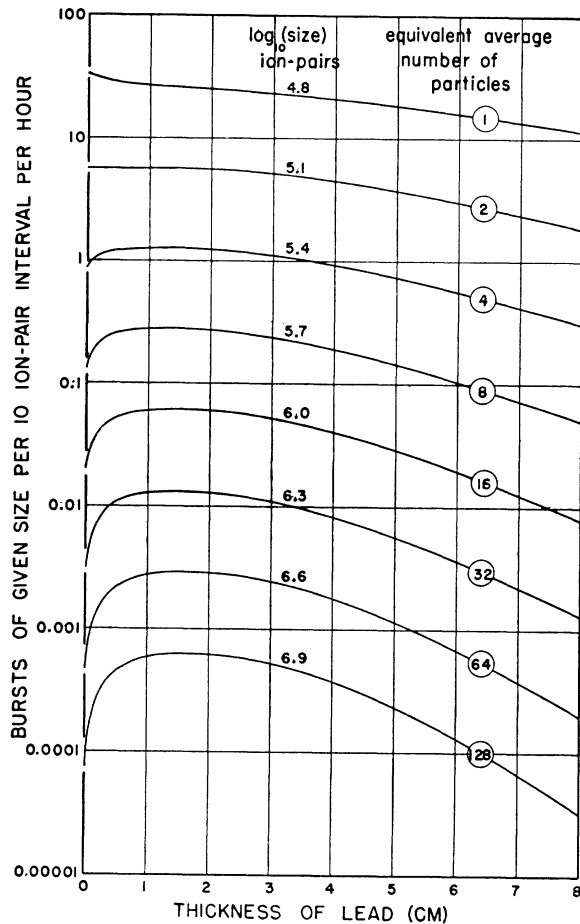


FIG. 9. The rates of occurrence per hour per 10^6 ion-pair size interval of air-shower bursts of different given sizes as a function of thickness of the lead shield. The circled numbers on the curves indicate the average numbers of electrons crossing the ion chamber (area 324 cm^2).

process as described in Sec. 4(a) is indicated by the transition curves of Fig. 9. These curves show (a) a finite number of bursts of all sizes even with no lead, (b) a broad maximum which occurs at the same depth whatever the size of the bursts, (c) a strong increase in the height of the maximum with increasing size of burst, and (d) no increase to a maximum for bursts produced by single particles crossing the ion chamber. These features seem to be in qualitative agreement with what might be expected for bursts produced by extensive air showers, and the contrast with the curves of Fig. 6 should be noted.

(c) Electromagnetic Cascade Bursts

The calibration of the ion chamber, as described in 5(a) above, in terms of the average burst size produced by a particle at minimum ionization, enables the curves of Fig. 6 to be labeled with the average numbers of electrons crossing the ion chamber. Every third curve has been so labelled. The last point on each of these

curves at 27 cm of lead, is derived from a power-law differential size-frequency distribution (Table III, column 5) with exponent -2.73 . It is useful to normalize these rates to unity at 27 cm of lead and replot the curves using a linear ordinate scale. The result is shown in Fig. 10 where the curves are seen to be similar to the well-known Rossi curve² obtained with counters.

It is generally accepted that the Rossi curve includes showers of three main types: (1) electron-photon cascades arising from incident electrons and photons of the so-called soft component; these cascades, which we shall call the soft-component cascades, produce the initial maximum and are completely absorbed in about 12 cm of lead; (2) electron-photon cascades originating in the lead from the radiation and knock-on interactions of mesons; these build up in number within the first 12 cm of lead to a rate which then decreases very slowly with increasing thickness; and (3) penetrating showers and electron-photon cascades originating from nuclear interactions within the lead; at sea level these latter showers are thought to be much less frequent than those of types (1) and (2).

In Fig. 11 the transition curve for cascades of 32 particles has been replotted over the whole 27 cm of lead. The broken line indicates the growth of bursts from showers that originate within the lead. The very small rate of absorption of all bursts observed under more than 10 cm of lead (mean free path greater than 2000 g/cm^2) indicates that they arise mainly from the secondary effects of μ mesons and not from the nucleon component.

The existence of a second maximum⁶ in the Rossi curve at about 15 or 20 cm of lead has often been claimed—the present observations show no trace of such a maximum for any of the larger burst sizes. A small effect for bursts of only 2 or 3 particles, if it did exist, might not have been detected in the present experiment because of the masking effect of the large numbers of bursts of this size arising from single mesons and protons.

The transition curves of the bursts arising from the soft component (see Figs. 10 and 11) are quite different in character from those of the extensive air shower bursts (Fig. 9). The soft component bursts in fact seem to arise mainly from *single* electrons or photons incident on the lead shield. This conclusion is supported by the following facts: (1) The soft component electrons in the unshielded ion chamber have a size-frequency distribution curve (see Fig. 4 of I or Fig. 5 of this paper) very similar to that of the μ mesons which are known to be single; there is no evidence of incident electron showers of more than 2 or 3 electrons except those associated with extensive air showers. (2) The larger bursts do not occur at all until an appreciable thickness of lead has been placed above the ion cham-

⁶ See B. Hodges and L. W. Morris, Phys. Rev. **102**, 1164 (1956) for the pertinent references.

FIG. 10. Selected curves from Fig. 6 re-plotted, using a linear ordinate scale and after normalization of the rates at 27 cm of lead to unity. These curves are closely analogous to the Rossi transition curve obtained with counters. In any one curve, all bursts are of the same size as measured in number of ion pairs produced in the ion chamber. The corresponding average numbers of electrons crossing the ion chamber is indicated by the circled figures on the curves.

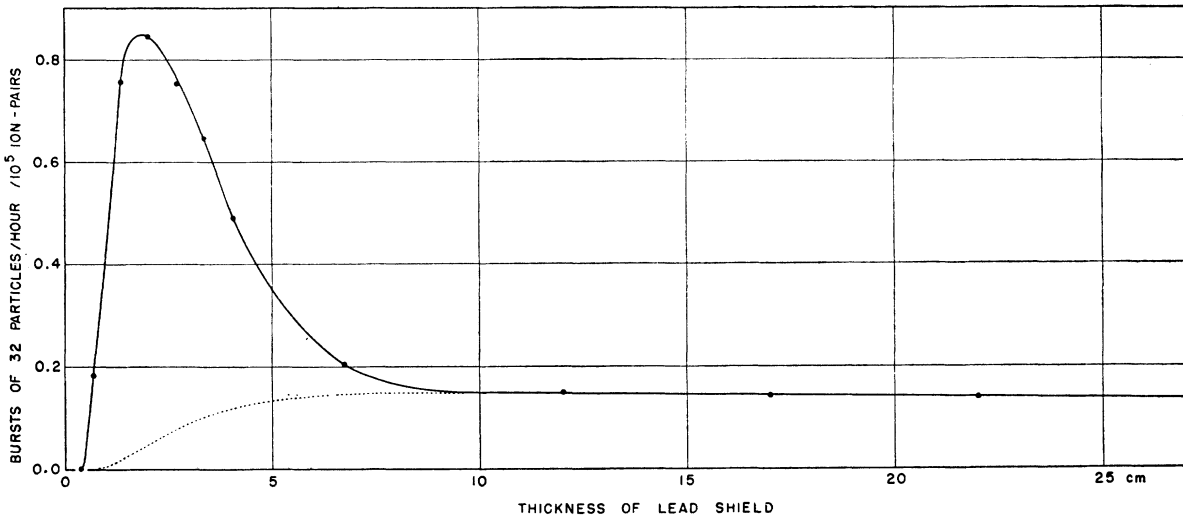
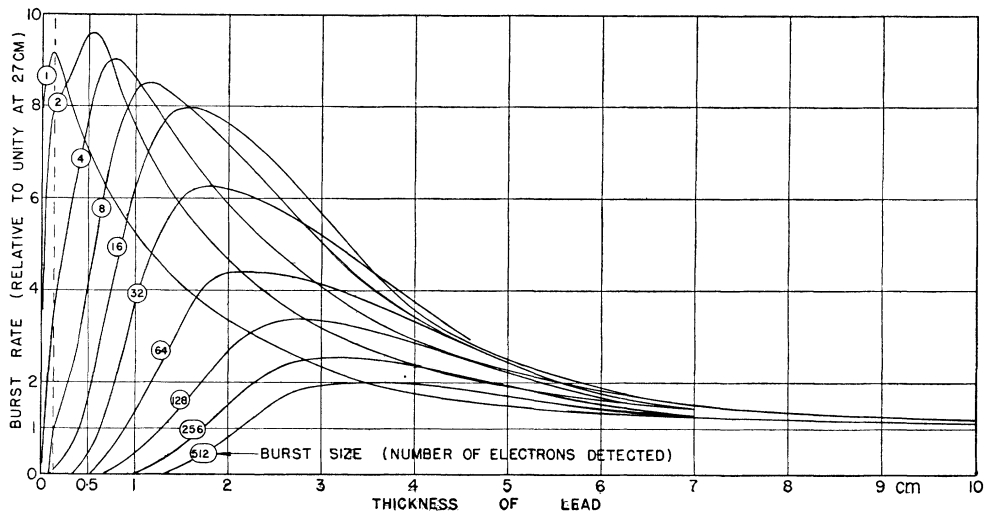


FIG. 11. The transition curve for bursts of 32 electrons, on the average, crossing the ion chamber. The broken curve indicates a separation between bursts arising from cascades produced by electrons or photons incident on the shield and bursts arising from cascades initiated within the shield (principally from μ mesons). There is no evidence of a second maximum at 15 or 20 cm of lead.

ber; it takes a certain thickness of lead to produce a moderately large burst if the cascade has to start from a single electron or photon. (3) The maximum of each curve is comparatively narrow and occurs at a progressively greater depth in lead as the size of the bursts increases, quite unlike the extensive shower transition curves which have a broad maximum, the position of which is insensitive to the thickness of the lead.

Attention is drawn to a peculiar feature of the transition curves of the soft component cascades associated with the first very thin (0.11-cm) lead shield. There is an anomalously large increase of the smaller bursts of one, two, and four particles best seen in Fig. 6. It is possible that this effect arises from materialization of photons of the soft component. Alternatively, it

quite possibly may have arisen from some error of the measurements or in the analysis.

The primary objective of this paper has been to present and analyze the experimental results. The transition curves of Fig. 10 are being discussed in more detail and compared with cascade theory in another paper now in preparation. It may be remarked that if these bursts do arise from isolated incident electrons or photons, the energies involved extend to some 50 Bev for cascades developing 500 particles at their maximum in lead.

ACKNOWLEDGMENT

We thank Miss Marjorie M. Hughes for her careful measurements of the pen recordings.